J Comp Physiol A (1991) 168:393–407

Journal of Comparative Physiology A Sensory, Neural, and Behavioral Physiology

Morphological correlates of pyramidal cell adaptation rate in the electrosensory lateral line lobe of weakly electric fish

Joseph Bastian* and Jay Courtright

Department of Zoology, University of Oklahoma, Norman, OK 73019, USA

Accepted January 10, 1991

Summary. 1. Extracellular HRP injections into the nucleus praeeminentialis dorsalis (NPd) of *Apteronotus leptorhynchus* retrogradely labeled a population of electrosensory lateral line lobe (ELL) efferent cells, deep basilar pyramidal cells, that differ morphologically from the previously described basilar and nonbasilar pyramidal cells. These neurons are found deep in the ELL cellular layers; they have small cell bodies and very short sparsely branching apical dendritic trees. The previously described basilar and nonbasilar pyramidal cells are larger, have extensive apical dendrites and are found more superficially.

2. Axon terminals of the deep basilar pyramidal cells were recorded from in the NPd and labeled with lucifer yellow. These NPd afferents have high, regular spontaneous firing rates, and respond tonically to changes in electric organ discharge amplitude.

3. Deep basilar pyramidal cell bodies were recorded from and labeled in the ELL, and these showed the same physiological responses as did the NPd afferent fibers.

4. In addition, basilar pyramidal cells were found which had spontaneous activity patterns and adaptation characteristics intermediate to those typical of the superficial basilar pyramidal cells and the deep basilar pyramidal cells. The size of the pyramidal cells' apical dendritic trees and the placement of their somata within the dorsoventral extent of the ELL cellular layers are highly correlated with the neurons' physiological properties.

Key words: Electroreception – Descending control – Adaptation – Pyramidal cells – Weakly electric fish – Sensory processing

Abbreviations: *BP* basilar pyramidal cell; *DBP* deep basilar pyramidal cell; *EGp* eminentia granularis posterior; *ELL* electrosensory lateral line lobe; *EOD* electric organ discharge; *GABA* gamma amino butyric acid; *HRP* horseradish peroxidase; *NBP* non basilar pyramidal cell; *NMDA* N-methyl-D-aspartate; *NPd* nucleus praeeminentialis dorsalis; *PSTH* post stimulus time histogram; *TSF* tractus strati fibrosi

* To whom offprint requests should be sent

Introduction

The electrosensory lateral line lobe (ELL) of gymnotiform fish, the primary processing region for the electric sense, is rapidly becoming one of the most thoroughly understood components of any vertebrate nervous system. The ELL is a laminated structure containing at least 11 cell types, and is the sole recipient of the electroreceptor afferent projection (Réthelyi and Szabo 1973; Maler et al. 1981). The structure is divided into 4 contiguous subdivisions or segments, each having the same lamination pattern and containing all of the major cell types. The most medial ELL segment receives somatotopic input from the ampullary category of electroreceptors and processes information about low-frequency electrical signals encountered in the environment. Each of the remaining 3 segments, referred to as the lateral, centrolateral, and centromedial, receives a complete somatotopic projection of the tuberous electroreceptor afferents (Heiligenberg and Dye 1982; Carr et al. 1982). The tuberous electroreceptors encode information about the animal's electric organ discharge (EOD) and there are two subtypes. The 'P-type' tuberous receptors respond to changes in the amplitude of the animal's electric organ discharge (EOD), while the 'T-receptors' encode timing information. The T receptor primary afferents synapse primarily on ELL spherical cells which project to the torus semicircularis and provide timing information critical for the jamming avoidance behavior (see Heiligenberg 1986 for review). The P receptor primary afferents make excitatory synapses with a second category of ELL output neuron, the basilar pyramidal cells (BP), and also make excitatory synapses with the ELL granule interneurons. These interneurons inhibit a third type of ELL output neuron, the nonbasilar pyramidal (NBP) cell (Maler et al. 1981). The basilar and nonbasilar pyramidal cells, also referred to as E- and I-cells, respond to increased afferent input with excitation and inhibition, respectively. Both the BP and NBP cells project to the torus semicircularis (TS) and to an

isthmic structure, the n. praeeminentialis dorsalis (NPd) (see Carr and Maler 1986; Zakon 1986; Bastian 1986c, 1990 for reviews).

In addition to receiving the electroreceptor afferent input, the ELL receives massive descending inputs, principally from the n. praeeminentialis. Output neurons of the NPd project bilaterally via the tractus strati fibrosi (TSF) to the ELL and form its ventral molecular layer (Sas and Maler 1983). Nucleus praeeminentialis efferent fibers also project bilaterally to a mass of granule cells, the posterior eminentia granularis (EGp), which lies dorsal to the ELL molecular layers (Sas and Maler 1983, 1987). The EGp granule cell axons form a very dense projection of cerebellar-like parallel fibers which constitutes the ELL dorsal molecular layer. Both the basilar and nonbasilar pyramidal cells, as well as several types of interneurons, have large apical dendritic trees which ramify within both the ventral and dorsal molecular layers (Maler 1979; Maler et al. 1981; Saunders and Bastian 1984). Hence, these ELL output cells are not only expected to respond to electroreceptor afferent input, but also to be sensitive to patterns of descending activity originating in the NPd.

Initial experiments aimed at determining the role of these descending or feedback inputs to the ELL used microinjection of local anesthetic or small lesions of the EGp to interrupt input to the ELL dorsal molecular layer. These manipulations lengthened the BP and NBP neurons' adaptation time constants, increased the cells' sensitivity to EOD amplitude changes by up to 300%, and increased receptive field size (Bastian 1986a). A subsequent study indicated that one role for the descending activity in the NPd–EGp–DML pathway was to provide a means for adjusting the gain or sensitivity of ELL output neurons to compensate for global changes in EOD amplitude (Bastian 1986b).

An important function of the electrosensory system is to enable the animals to sense, identify and orient to objects in their environment independent of visual or normal lateral line cues. Objects differing in impedance from the surrounding water distort the EOD field and thus cause changes in the activity of electroreceptor afferents. The amplitude of the distortion, or change in EOD voltage sensed by the receptors, is a function of EOD amplitude, of the difference in conductivity between the electrolocation target and the water, and of the distance between the fish and the target (Heiligenberg 1977; Bastian 1981a, 1986c, 1990). In normal fish, large reductions in EOD voltage result in little or no change in the responses of ELL output neurons to a standard electrolocation target despite the fact that changes in afferent input are reduced. If, however, input to the ELL dorsal molecular layer is interrupted, then, although the sensitivity of BP and NBP cells is increased, reductions in EOD voltage result in significant reductions in the responses of ELL basilar pyramidal cells to the standard target (Bastian 1986b). These results suggest that the input descending via the EGp mediates an inhibition of the ELL output neurons and that this inhibition can be reduced when the system senses decreased EOD amplitude, thereby increasing gain and maintaining near constant responses to electrolocation targets. Experiments in which the GABA antagonist bicuculline is microinjected into the ELL produce many of the same effects that result from EGp lesions or anesthetic blockade (Shumway and Maler 1989).

In order for the system to be able to compensate for changes in the strength of the EOD, some measure of EOD amplitude must be continuously available. Neurons have been found within the NPd, the multipolar cells described by Sas and Maler (1987), which encode EOD amplitude tonically and with high resolution (Bastian and Bratton 1990). Intracellular recording and lucifer yellow labeling of multipolar cells in the NPd and of their axon terminals, as well as the results of retrograde labeling studies (Sas and Maler 1987), demonstrate that these cells project to the EGp. The existence of these tonically responding NPd cells raises the question of their source of input. The ELL is the only recipient of the electroreceptor afferents, and it projects to the NPd directly as well as indirectly via the torus semicircularis (Sas and Maler 1983). However, tonically responding ELL output neurons have yet to be described. Both the basilar and nonbasilar pyramidal cells rapidly adapt to long term changes in EOD amplitude (Bastian 1981b, 1986a, b; Saunders and Bastian 1984; Shumway 1990a). Enger and Szabo (1965) did describe a category of tonically responding units but these were found more superficially, probably within the EGp, and may have been axon terminals of the NPd multipolar cells. Axon terminals having tonic response characteristics similar to those of the NPd multipolar cells have also been filled in the caudal regions of the NPd. It was suggested that these are axons of an additional category of ELL output neuron having nonadapting response characteristics (Bastian and Bratton 1990).

The present study was undertaken to determine if tonically responding output neurons could be found within the ELL, and if so, to determine if these had morphological characteristics different than those of the previously described basilar and nonbasilar pyramidal cells. Extracellular injection of HRP into the caudal nucleus praeeminentialis retrogradely labeled a morphologically distinct population of ELL efferent neurons, the deep basilar pyramidal cells. Intracellular recording and labeling with lucifer yellow verified that these cells had the tonic response properties predicted for this type of ELL output neuron. Additionally, we found that several measures of basilar pyramidal cell physiological characteristics were highly correlated with both the size of the neurons' apical dendritic tree and with the placement of their somata within the ELL cell layers.

Materials and methods

The weakly electric fish *Apteronotus leptorhynchus*, the brown ghost knife fish, was used exclusively in these studies. Surgical techniques were the same as described earlier (Bastian 1981a).

Anatomical studies. Animals were anesthetized by immersion in a solution of tricaine methane sulfonate (MS222, Sigma) and artifici-

ally respirated with this same solution. A small region of skull overlying the optic tectum was removed and a micropipette with a tip diameter of 10 to 20 μm containing a 10% solution of HRP (Sigma type IV, dissolved in 0.1 *M* tris, pH 7.4) was inserted into the NPd or torus semicircularis. Horseradish peroxidase was iontophoretically injected by passing 10 s positive current pulses of approximately 5 μA for periods of from 10 to 30 min. The opening in the skull was covered with a mixture of gelfoam and petroleum jelly, and the skin was closed with 10–0 ophthalmological sutures. After a 3 to 4 day survival, the animals were deeply anesthetized with Ketamine and perfused with heparin Ringer solution, followed by 4% glutaraldehyde in phosphate buffer, followed by 30% sucrose. Sixty μm frozen sections were cut and processed for peroxidase with a DAB glucose-oxidase procedure (Metcalf 1985) and counterstained with pyronin yellow.

Physiological studies. For intracellular experiments animals were suspended in a tank, measuring 30 × 30 × 7 cm deep, mounted on a vibration isolation table. Fish were artificially respirated by a continuous flow of water over the gills, and water temperature and conductivity were held at 26 to 28 °C and 10 kΩ · cm, respectively.

Intracellular recordings were made with microelectrodes filled with a 10% solution of Lucifer yellow CH (Sigma) in 0.1 *M* LiCl. Pipettes were pulled from thin wall aluminosilicate glass and had an initial resistance in excess of 1000 MΩ. These were beveled in a jet stream containing 0.05 μm gamma alumina particles and had a final resistance of between 100 and 400 MΩ. Intracellular data were stored on magnetic tape (Hewlett Packard 3960, 3.75 ips, FM mode). Dye was ejected from the recording electrode with a bridge amplifier using either a steady hyperpolarizing current, 250–500 pA, or a negatively DC offset sinewave, 0.5–1 nA p-p. Animals were perfused with heparinized Ringer solution, followed by 4% paraformaldehyde in phosphate buffer, followed by 30% sucrose in 4% paraformaldehyde within 30 min after filling a neuron. Brains were mounted in gelatin and sectioned at 60 μm with a freezing microtome. Sections were viewed with a fluorescence microscope equiped with a low-light silicon intensified (SIT) television camera. Images were recorded on video tape and later replayed for reconstruction and morphological analysis. In a limited number of experiments single neurons were filled with HRP rather than lucifer yellow, and in these cases brains were processed as described for the anatomical studies.

The apteronotids have an electric organ derived from spinal motoneurons, hence their electric organ discharge remains normal even when they are immobilized with the curare-like drug gallamine triethiodide (Flaxedil). The discharge was recorded via electrodes placed near the animal's head and tail, and this signal was used to trigger single cycles of a sinusoidal signal having a period slightly less than that of the EOD. Step changes in EOD amplitude were produced by adding or subtracting this sinusoid from the animal's discharge. The amplitude of this stimulus was 0.375 mV/cm rms unless indicated otherwise. Electrical stimuli were isolated from ground via stimulus isolation transformers and were applied to the fish with electrodes mounted on the tank walls on either side of the fish ('transverse geometry') or with electrodes in the animal's mouth and at the tip of the tail ('symmetrical geometry'). With the former geometry, current flow is inward through one side of the body and outward through the opposite side, and changes in EOD amplitude of opposite sign occur on opposite sides of the body. With symmetrical geometry, current flow is unidirectional around the perimeter of the fish, hence changes in EOD amplitude of the same sign occur over about the rostral 80% of the body surface. EOD amplitude was measured with a pair of silver wire electrodes separated by 1 cm and oriented perpendicularly to the long axis of the fish just caudal to the operculum.

Data analysis. A neuron's spontaneous firing frequency was determined from the mean of interval histograms in which 200 to 500 consecutive spike intervals were accumulated, and the shape of the interval histograms was quantified by calculating the skewness coefficient, g1 (Sokal and Rohlf 1981). Responses to changes in electric organ discharge amplitude were summarized in raster displays or as plots of spike frequency versus time. In the latter case, spike frequency was determined from the number of spike intervals, including fractions, occurring during each consecutive 100 ms epoch of the spike record. The plots of spike frequency were typically smoothed with a simple digital filter to reduce random fluctuations (Bastian 1986b). Adaptation time constants were determined from the first 10 spike frequency measurements following a change in EOD amplitude. Time constant was calculated as the negative reciprocal of the slope of the best-fit line relating the natural log of spike frequency to elapsed time.

Results

Retrograde labeling of ELL output neurons

Small injections of HRP into the caudal regions of the NPd retrogradely label a uniform population of ELL output neurons having morphological characteristics significantly different from those of previously described ELL pyramidal cells. An example of an HRP injection is shown on the right side of Fig. 1A, and examples of the retrogradely labeled ELL neurons, which we will call deep basilar pyramidal cells (DBP), are shown in Fig. 1B and 2C. The majority of cells labeled as a result of injections into the ventral portion of the NPd (89%) were found in the centromedial segment of the ELL as is expected given the results of Maler et al. (1982), and as was seen in these earlier studies, anterogradely labeled fibers were found in the major efferent targets of the NPd: the EGp and the ELL ventral molecular layers (arrows in Fig. 1B). More dorsal NPd injections predominantly labeled cells in the lateral and centrolateral segments confirming the previously described topography of the ELL-to-NPd projection.

The retrogradely labeled ELL neurons project bilaterally to the NPd. Unilateral HRP injections such as that shown in Fig. 1A labeled 272 ELL neurons in two fish, and 59% of these were found in the contralateral ELL, and 41% were found ipsilaterally. Axon branches ascending to the NPd contralateral to the injection site were also well filled as is shown by the dense collection of filled fibers in the NPd on the left side of Fig. 1A and in Fig. 2A. Filled fibers were also found in the torus semicircularis ipsilateral and contralateral to the injection site.

The relative positions of all retrogradely labeled somata within the cellular laminae of the ELL resulting from injections into the ventral NPd in two fish are shown in Fig. 3A, B. The labeled neurons were found in a relatively narrow band within the granule cell lamina just below the plexiform layer, typically at a level between 20 and 40% of the total thickness of the cell layers. Soma width averaged 8.5 μm, and virtually all of the labeled cells had a basilar dendrite which extended into the deep fiber layer. The apical dendrites of these cells were very short and sparsely branched; they traversed the ELL ventral molecular layer, but did not extend through the dorsal molecular layer (Figs. 1B, 2C).

In an earlier study, Maler et al. (1982) also used retrograde transport of HRP injected into the NPd or the TS to identify ELL efferent neurons. Their results dif-

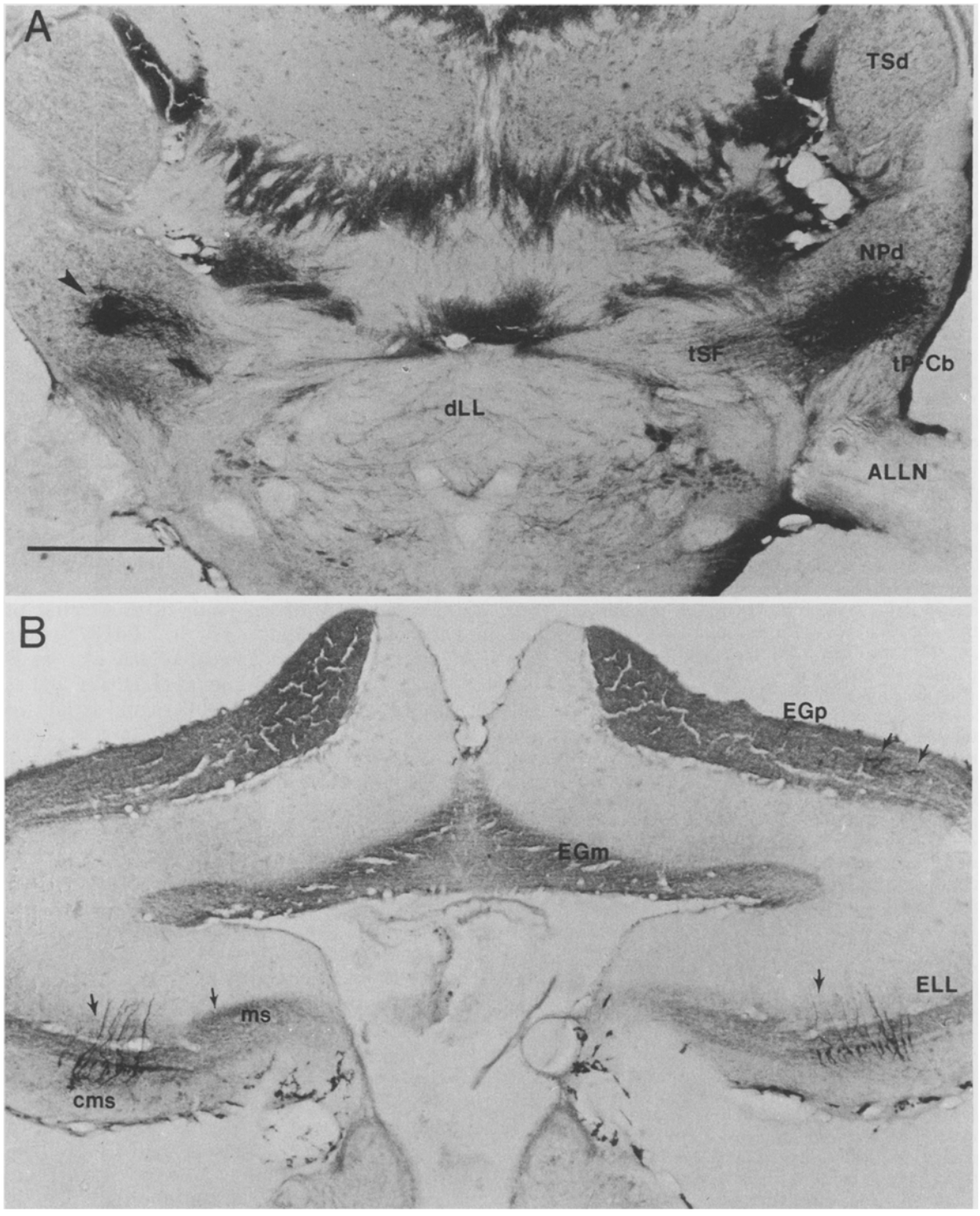

Fig. 1. A Transverse section through the brain at the level of the caudal NPd showing an HRP injection site on the right side. The arrowhead on the left side indicates a cluster of NPd afferent fibers which are branches of axons of the bilaterally projecting ELL cells retrogradely labeled by this injection. **B** Transverse section through the caudal ELL showing the bilateral population of deep basilar pyramidal cells labeled by the NPd injection. The arrows in the EGp show anterogradely filled NPd efferents terminating in this structure, and the arrows in the ELL molecular layers show anterogradely labeled VML fibers within both the centromedial and medial segments. Calibration bar in **A** and **B** 500 μm. *ALLN*, anterior lateral line nerve; *cms*, centromedial segment; *dLL*, decussation of the lateral lemniscus; *EGm*, medial eminentia granularis; *EGp*, posterior eminentia granularis; *ELL* electrosensory lateral line lobe; *ms*, medial segment; *NPd*, nucleus praeeminentialis dorsalis; *tP–Cb*, tractus praeeminentialis cerebellaris; *TSd;* torus semicircularis dorsalis; *tSF*, tractus strati fibrosi

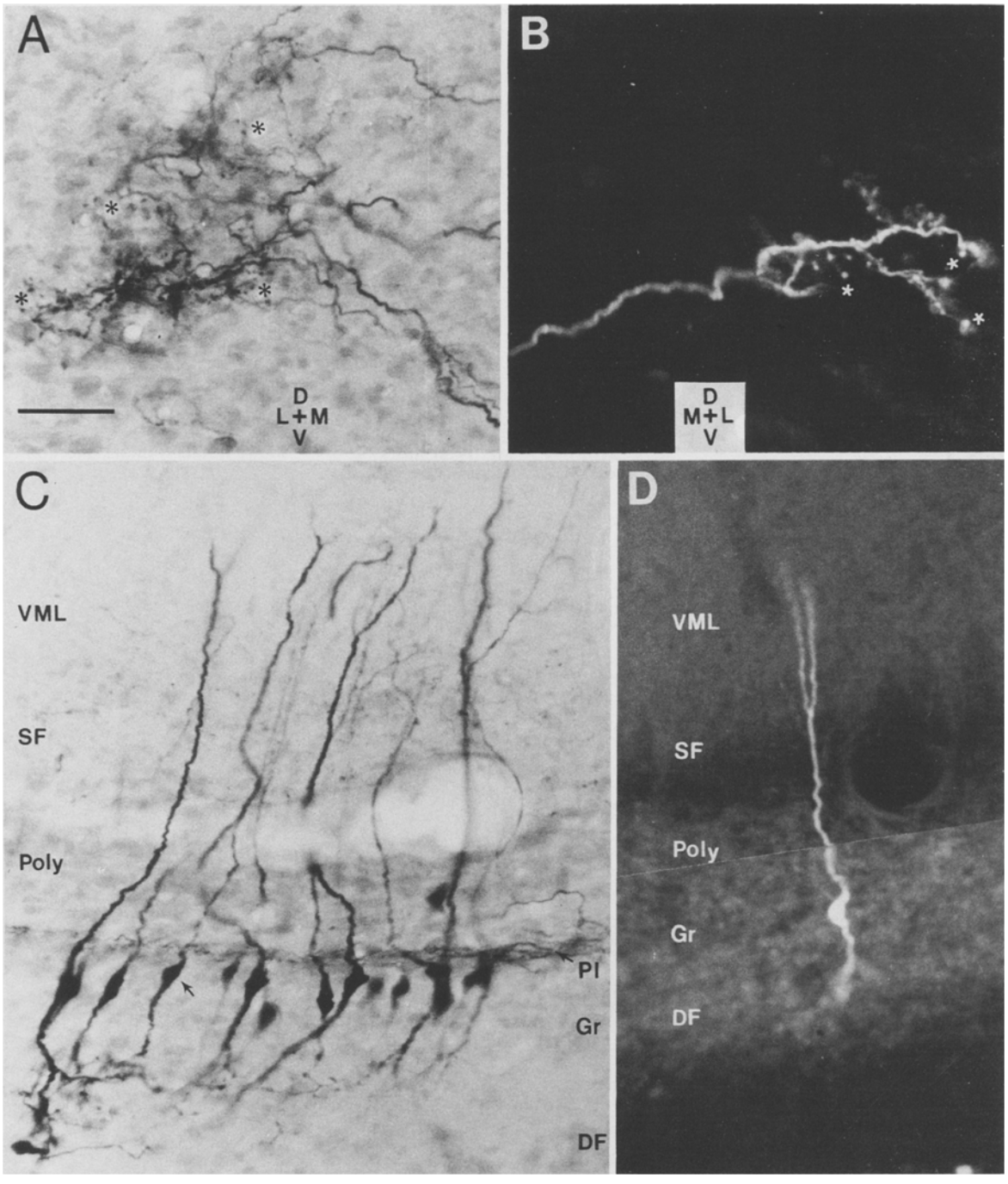

Fig. 2. A Higher magnification view of the NPd afferents terminating contralateral to the NPd injected with HRP. Asterisks show varicosities typically found along the terminal branches of these axons. **B** Portion of a lucifer yellow filled NPd afferent axon, asterisks show varicosities typical of these terminal branches. **C** Higher magnification view of the cluster of retrogradely labeled deep basilar neurons of the ELL shown on the left of Fig. 1B. **D** Lucifer yellow filled deep basilar pyramidal cell. The calibration bar in **A:** 50 μm holds for **B–D.** *DF,* deep fiber layer; *Gr,* granule cell layer; *Pl,* plexiform layer; *Poly,* polymorphic cell layer; *SF,* stratum fibrosum; *VML,* ventral molecular layer

fered, however, in that a more heterogeneous population of ELL neurons was labeled. Both basilar and nonbasilar pyramidal cells were identified, cell bodies were distributed throughout the more dorsal regions of the cellular layers, and the neurons had much larger apical dendritic trees which branched profusely and extended through the entire thickness of the dorsal molecular layer. These authors mentioned the existence of deeper cell types and they speculated whether these were ventrally displaced pyramidal cells or perhaps an additional category of ELL output neuron.

We made HRP injections into more rostral and more dorsal regions of the NPd and into the TS in order to determine if the preferential labeling of the DBP neurons

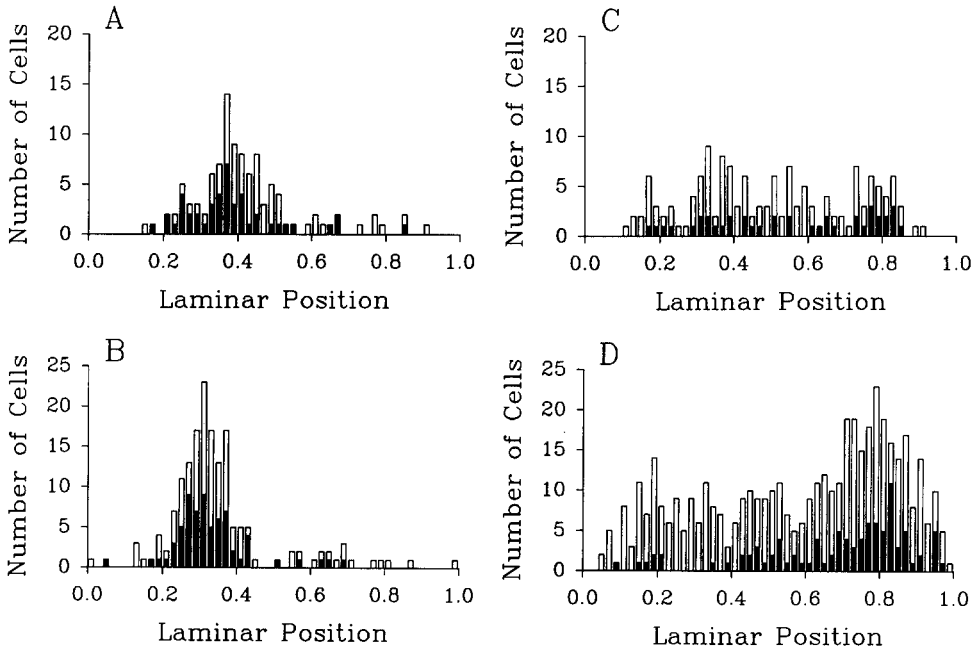

Fig. 3A–D. Histograms summarizing the distributions of positions of retrogradely labeled cell bodies within the cellular layers of the ELL following HRP injections to the NPd or TS. Laminar position of 0.0 corresponds to the ventral border of the granule cell layer, and position 1.0 indicates the dorsal boundary of the polymorphic cell layer. Filled bars indicate cells in the ELL ipsilateral to the injection site, open bars indicate contralateral cells. **A, B** Results from injections such as that shown in Fig. 1A. **C** Summarizes results from a more dorsal and rostral NPd injection, and **D** shows results from an injection to the central TS

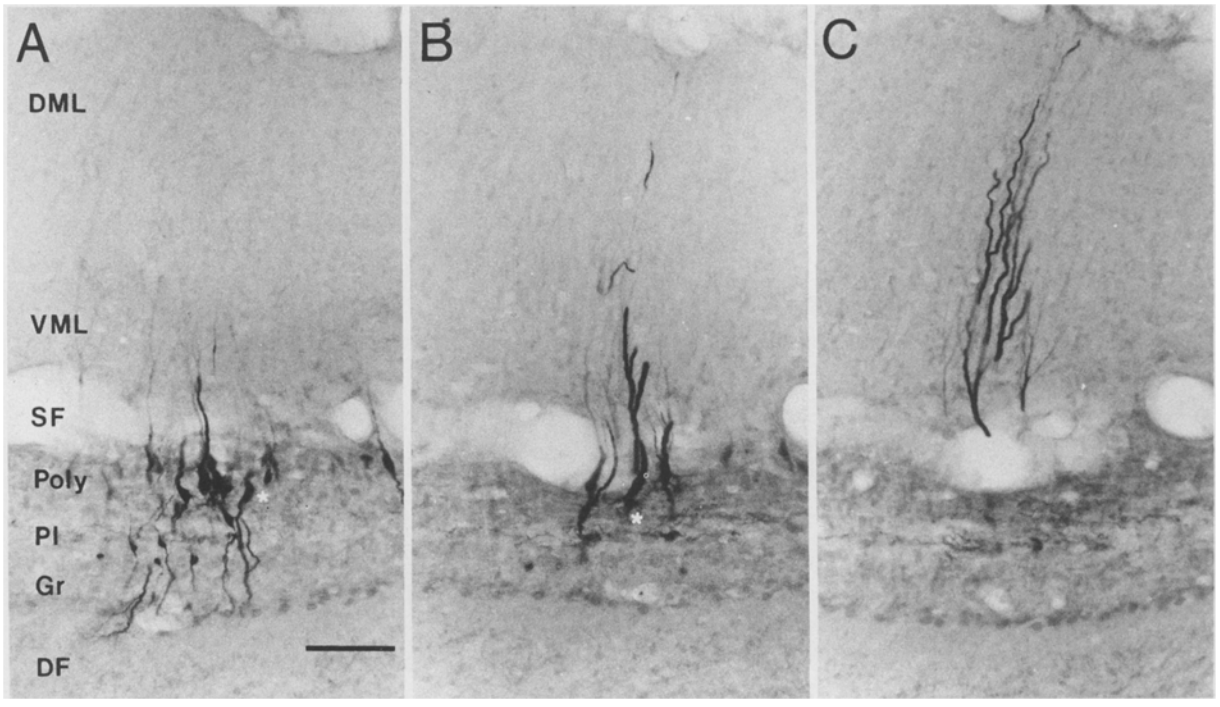

Fig. 4A–C. Retrogradely filled neurons within the centromedial segment of the ELL resulting from an HRP injection to the contralateral torus. **A–C** are from 3 consecutive sections. Both deep and more superficial cells are labeled in **A. B** and **C** show the very large apical dendrites, typical of the superficial pyramidal cells, extending through the dorsoventral extent of the DML. Asterisks in **A** and **B** show basilar and nonbasilar pyramidal cells, respectively. Calibration in **A** 100 μm and holds for **B, C.** *DF,* deep fiber layer; *DML,* dorsal molecular layer; *Gr,* granule cell layer; *Pl,* plexiform layer; *Poly,* polymorphic cell layer; *SF,* stratum fibrosum; *VML,* ventral molecular layer

was correlated with the site of HRP injection. The laminar distribution of labeled cells resulting from a dorsal NPd and central torus injection are shown in Fig. 3C, D, respectively. Both experiments restulted in a more heterogeneous population of labeled neurons, and many cell bodies were found above the plexiform layer in the polymorphic layer. In the case of the torus injections, the more superficial cells were intensely labeled revealing the full extent of their apical dendritic trees, but the apical dendritic trees of these superficial cells were never well filled following NPd injections. Figure 4A–C shows a portion of the centromedial segment from 3 consecutive

sections of the ELL contralateral to an HRP injection in the torus. The superficial cells as well as smaller deep cells are filled (Fig. 4A), and, among the former, both basilar (asterisk in Fig. 4A) and nonbasilar (asterisk in Fig. 4B) types are seen. The apical dendrites of the more superficial cells, typical basilar and nonbasilar pyramidal cells, traverse the full extent of the dorsal molecular layer (Fig. 4C) as compared to the apical dendrites of the deep cells shown in Figs. 1B and 2C. The more dorsal NPd injections and the torus injections also resulted in fewer ELL cells ipsilateral to the injection site being labeled, 27% and 21% respectively. Torus injections typically resulted in labeled cells within all 4 ELL segments, branches of the retrogradely labeled ELL efferent axons projected to the ipsilateral and contralateral NPd's, and anterograde labeling of torus efferent axons were seen in the ipsilateral NPd, as previously described (Carr et al. 1981; Maler et al. 1982; Carr and Maler 1986).

Soma size varied with a cell's position within the cellular laminae, and those found in the granule cell layer were smaller than those in the polymorphic layer. Volume was calculated from measurements of length and width assuming an ellipsoid shape. Soma volumes of the cells of Fig. 3D located above the plexiform layer, laminar positions 0.5 and above, averaged 11,316 μm^3 ($n = 292$, SE = 450) and were significantly larger than those found deeper than a laminar position of 0.5 (mean = 5,115 μm^3, $n = 173$, SE = 313). The volume of the cells labeled following the ventral NPd injections, those of Fig. 3A, B, averaged 6,099 μm^3 ($n = 272$, SE = 206). These were also significantly larger than the deeper cells labeled by torus injections ($P = 0.01$, t-test).

These anatomical observations suggest that there is a fourth category of ELL output neuron, the deep basilar pyramidal cells, in addition to the previously described spherical cells, basilar pyramidal cells, and nonbasilar pyramidal cells. These are found in the granule cell layer and have basilar dendrites extending into the deep fiber layer, hence they probably receive direct receptor afferent input. Their soma volume is roughly half that of the basilar and nonbasilar pyramidal cells and these neurons have much smaller apical dendritic trees. The DBP cells project bilaterally to the NPd and the torus semicircularis, and they may provide the predominate input to the caudal ventral NPd. However, the DBP cells also project to the more dorsal and rostral regions of the NPd. Injections of wheat germ agglutinin HRP that involve most of the NPd clearly label the deep population as well as neurons within the polymorphic layer throughout the rostrocaudal extent of the lateral, centrolateral and centromedial segments (Maler, personal comm.).

Physiological properties of NPd afferent fibers

Afferent fibers are often impaled when intracellular recordings are made from the caudal NPd, and the activity patterns of these afferents differ significantly from those typical of the basilar and nonbasilar pyramidal cells in the ELL (Bastian and Bratton 1990). A portion of a lucifer yellow filled NPd afferent fiber is shown in Fig. 2B. The filled axon enters the nucleus from its medial boundary and, after reaching the caudal-ventral region, branches into a terminal field. The terminal fibers have a beaded appearance due to large numbers of varicosities (asterisks, Fig. 2B) similar to those seen in anterogradely labeled fibers resulting from extracellular HRP injections (asterisks in Fig. 2A). In the strongest lucifer yellow fills, the axon could be traced within the lateral lemniscus to the plexiform layer of the ELL, but labeling was never sufficient to reveal the cell body.

The physiological properties of the fiber of Fig. 2B are summarized in Fig. 5. The spontaneous firing frequency of this fiber, with the EOD amplitude at its normal value, averaged 38.9 spikes/s (Fig. 5B), a value somewhat lower than the average of 53.9 ± 5.6 spikes/s for the sample of 6 fibers studied. Interval histograms of this activity were always bell shaped. Histograms of basilar or nonbasilar pyramidal cells' activity are highly skewed to the right (Fig. 8A) because the BP and NBP cells tend to fire short bursts of spikes separated by longer intervals. The skewness of interval histograms was measured by computing the moment statistic, g1, which is zero for normal distributions, positive for those skewed to the right and negative for those skewed to the left. This statistic averaged 0.21 ± 0.08 for the 6 NPd afferent fibers that were labeled.

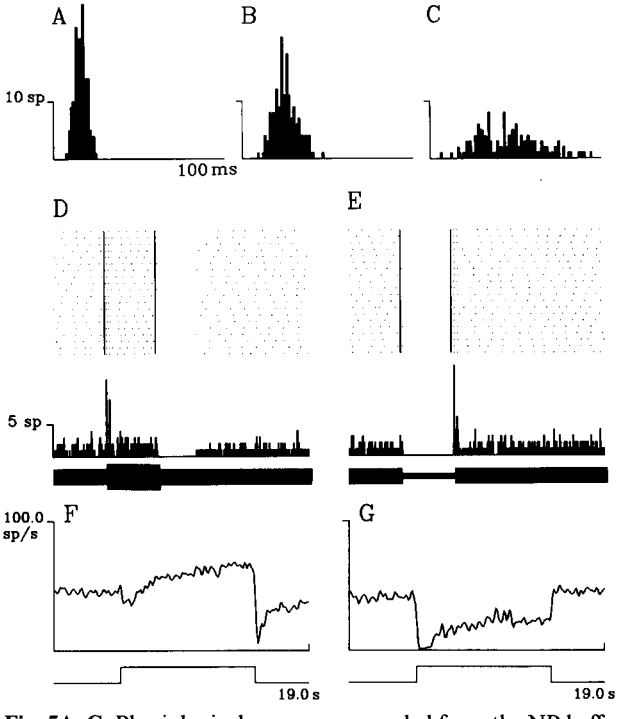

Fig. 5A–G. Physiological responses recorded from the NPd afferent fiber shown in Fig. 2B. **A–C,** spike interval histograms of spontaneous activity (**B**) and of responses to 1.2 mV/cm rms increases (**A**) and decreases (**C**) in EOD amplitude. Average frequencies in spikes/s and skewness coefficients were 62.4 and 0.04, 38.9 and 0.31, 19.1 and 0.41 for A–C, respectively. The raster displays and PSTHs of **D, E** show the fiber's responses to 100 ms increases and decreases in EOD amplitude of 1.2 mV/cm rms. The frequency versus time plots of **F, G** show the responses of this fiber to 10 s increases and decreases in EOD amplitude of 1.2 mV/cm rms, respectively. Stimuli were presented with transverse geometry, and for this fiber increased input to the contralateral ELL was an excitatory stimulus as was an EOD increase presented with symmetrical geometry

These fibers responded to brief, 100 ms, increases or decreases in EOD amplitude as shown in Fig. 5D, E respectively. The onset of a transversely applied stimulus, which increased the EOD amplitude on the side of the body contralateral to the NPd recorded from, evoked a brief burst of from 2 to 4 spikes followed by a much smaller frequency increase during the rest of the stimulus period. The opposite stimulus, a contralateral decrease in EOD amplitude, caused the cell to pause. Two of the 6 fibers studied responded in this manner, the remaining 4 were excited by ipsilateral EOD increases and inhibited by ipsilateral decreases. These differences are due to the bilateral projection pattern of the ELL output neurons. Based on the extracellular HRP injections it is nearly equally probable to record from an axon having its cell body, hence its receptor afferent input, ipsilateral or contralateral to a given NPd.

Figure 5F, G shows the changes in the fiber's firing frequency due to a 10 s increase and decrease in EOD amplitude, respectively. Following the initial burst or pause, the cell gradually adopted a new firing frequency which was maintained for the duration of the stimulus. These responses were completely tonic, no adaptation was seen. The interval histograms of Fig. 5A, C were made during the last 5 s of the responses shown in Fig. 5F, G respectively. Spike frequency increased from a resting value of 38.9 to 62.4 spikes/s and decreased to 19.1 spikes/s, and the histograms remained bell shaped. The initial burst response of these fibers is similar to the responses of the most phasic basilar pyramidal cells (Fig. 8B), however the BP cells adapt to prolonged changes in EOD amplitude within tens of milliseconds.

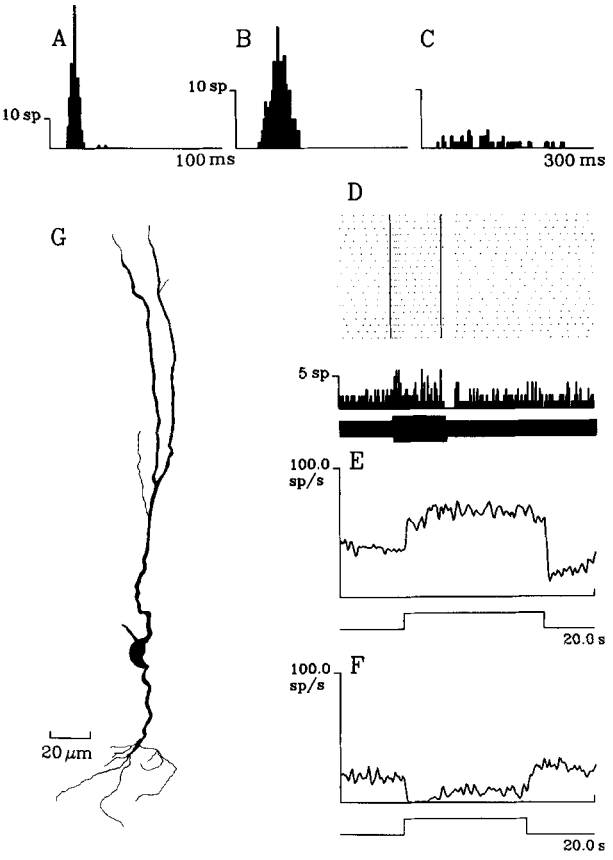

Fig. 6A–G. Physiological responses of the lucifer yellow filled deep basilar pyramidal cell of Fig. 2D. **A–C** Interval histograms of activity with 1.2 mV/cm rms increased EOD amplitude, normal EOD amplitude, and 1.2 mV/cm decreased EOD amplitude, respectively. Average firing frequencies and measures of skewness (g1) are 68.6 spikes/s and 0.12, 39.2 and −0.05, and 7.9 and 0.6. **D** Raster display and PSTH of the cell's responses to 100 ms increase in EOD amplitude, 1.2 mV/cm rms. **E, F** Responses to the same sized increase and decrease in EOD amplitude applied for approximately 10 s. All stimuli were applied with transverse geometry. **G** Reconstruction of this deep basilar pyramidal cell. The reconstruction of the basilar dendrite is incomplete

Physiological properties of ELL efferent neurons

Intracellular recordings with either Lucifer yellow or HRP filled pipettes were made to determine if the deep basilar pyramidal cells had physiological properties similar to those of the NPd afferent fibers described above. An example of a lucifer yellow filled DBP cell from the centromedial segment is shown in Fig. 2D. Soma size, position within the ELL, and apical dendritic size are similar to those of the cells filled by retrograde transport from the NPd (Fig. 2C). The physiological characteristics of this cell are summarized in Fig. 6 along with a more complete reconstruction. The spontaneous firing frequency averaged 39 spikes/s (Fig. 6B), and the interval histogram was symmetrical (g1 = −0.05). The responses to 100 ms increases in EOD amplitude showed the same brief initial burst followed by a weak increase in activity (Fig. 6D), and the cell was inhibited by reductions in EOD amplitude (not shown). This cell responded tonically to long-duration increases or decreases in EOD amplitude (Fig. 6E, F respectively), and the interval histograms produced during these tonic responses remained bell shaped (Fig. 6A, C).

Earlier studies showed that the basilar pyramidal cells produced phasic or rapidly adapting responses when stimulated with stepchanges in EOD amplitude (Enger and Szabo 1965; Bastian 1981; Saunders and Bastian 1984), and time constants of adaptation determined from PSTHs such as Fig. 6D were generally short; averaging about 25 ms (Bastian 1986a). More recently, Shumway (1990a), using extracellular methods, found that several physiological properties of pyramidal cells, including adaptation time constant, varied with the segment within which a neuron was found. Shorter adaptation time constants were found for lateral segment cells, longer for centrolateral, and longest for centromedial cells. We recorded from and labeled neurons within each of the 3 ELL segments showing widely different adaptation rates and spontaneous activity patterns to determine if these response characteristics were correlated with neuronal morphology or soma position within the ELL cell layers.

Reconstructions of lucifer yellow filled neurons spanning the range of morphological variation seen are shown in Fig. 7A–C. The neuron of Fig. 7A was located in the centrolateral segment at the top of the polymorphic layer (laminar position = 0.94), and its apical dendrite extended upward through the entire dorsal mole-

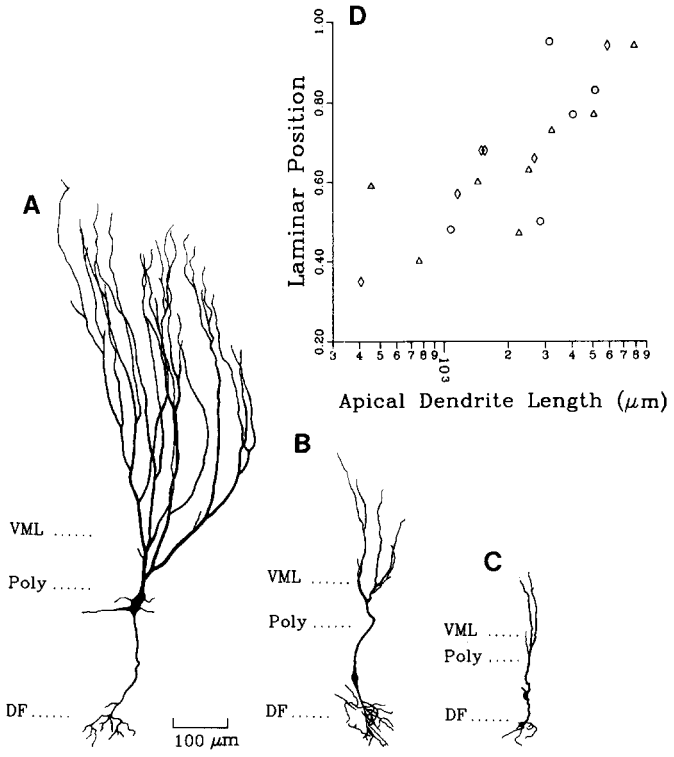

Fig. 7A–C. Examples of basilar pyramidal cells spanning the ranges of variability of apical dendritic size and soma depth within the cellular layers. Dendritic lengths and laminar positions for **A–C** are 7891 μm and 0.94, 1074 μm and 0.48, and 406 μm and 0.35, respectively. **D** Scatterplot of laminar position and apical dendrite length. Circles represent cells from the lateral segment; triangles, centrolateral segment cells; diamonds, centromedial segment cells. The correlation coeff. for all data was 0.77, and coeffs. for the lateral, centrolateral, and centromedial segments were 0.69, 0.70 and 0.96, respectively. *DF*, dorsal boundary of deep fiber layer; *Poly*, dorsal boundary of polymorphic cell layer; *VML*, ventral boundary of ventral molecular layer

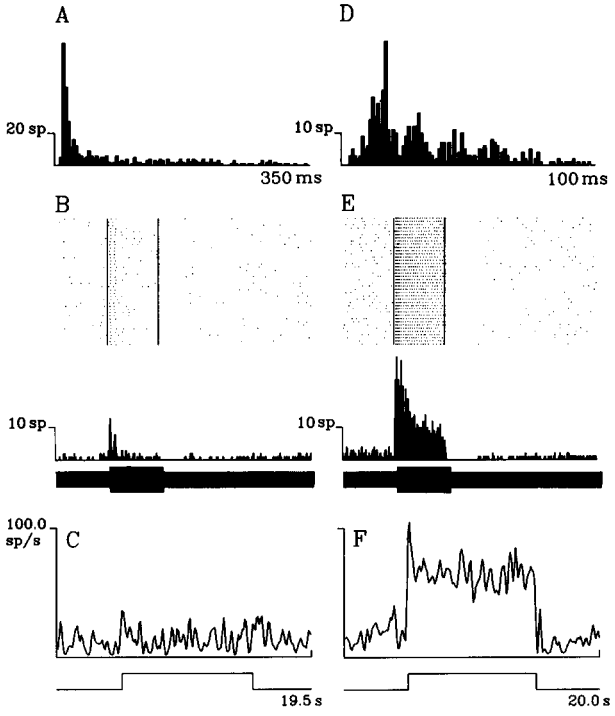

Fig. 8A–C and D–F. Physiological responses of the neurons of Fig. 7A and B, respectively. Spontaneous frequency and interval histogram skewness are 11.7 spikes/s and 1.29 for **A**, and 29.8 spikes/s and 0.95 for **D**. Adaptation time constants determined from the PSTHs of responses to 100 ms increases in EOD amplitude (**B, E**) are 1.9 and 50 ms. Responses to 10 s increases in EOD amplitude are shown in **C, F** and time constants determined from these data are 0.49 s and 2.25 s, respectively. Adaptation ratios for these responses, see text for explanation, are −0.05 and 0.52. Stimulus amplitude for **B** and **C** was 1.2 mV/cm rms

cular layer. The size of the apical dendrite was quantified by measuring the total length of all branches and was 7,891 μm for this cell. The neuron shown in Fig. 7B was located in the lateral segment, laminar position = 0.48, and its apical dendrite measured 1,074 μm. The neuron described in Fig. 6 is reproduced here (Fig. 7C) for comparison with these more typical basilar pyramidal cells. It was located at laminar position 0.35 in the centromedial segment, and its apical dendrite had a total length of 406 μm. The differences in the thickness of the laminae indicated in Fig. 7 reflect changes related to rostro-caudal position within the ELL and segmental variations. These reconstructions underestimate the complexity of the basilar dendrites because the high density of fine fibers made accurate reconstruction from lucifer fills virtually impossible. Figure 7D shows that the position of a neuron's soma within the cellular laminae and the size of its apical dendrite were strongly correlated. The correlation coefficients for the lateral (circles), centrolateral (triangles), and centromedial segment cells (diamonds) were 0.69, 0.70, and 0.96, respectively, and the coefficient for all data was 0.77.

Several physiological characteristics of the cells of Fig. 7A and B are summarized in Fig. 8A–C and D–F, respectively. The cell of Fig. 7A had low spontaneous firing frequency, 11.7 spikes/s, and the interval histogram (Fig. 8A) was skewed to the right (g1 = 1.29). The spontaneous firing rate of the cell of Fig. 7B was higher, 29.8 spikes/s, and the interval histogram of this data (Fig. 8D) was also skewed to the right, but less so (g1 = 0.95). These measures were made for all cells filled and are plotted as a function of the logarithm of total apical dendrite length in Fig. 9A, B. Spontaneous discharge rate was negatively correlated with dendrite length (r = −0.83), and this relationship was approximately the same for the samples of cells from each of the ELL segments (see legend of Fig. 9). Interval histogram skewness was also related to apical dendrite length (r = 0.63), hence, cells with small apical dendrites fired more regularly and at higher frequencies, while those with more superficially located somata and larger apical dendrites tended to fire brief bursts separated by longer intervals. The responses of the neurons of Fig. 7A, B to 100 ms increases in EOD amplitude are shown in Fig. 8B, E, respectively, and their responses to 10 s EOD increases are shown in Fig. 8C, F. The more superficial cell with the large apical dendrite responded phasically to both the brief and prolonged stimulus, and firing frequency quickly adapted to its resting discharge level. The neuron of Fig. 7B, with the intermediate sized apical dendrite, also showed a strong response to the onset of these stimuli, but the responses

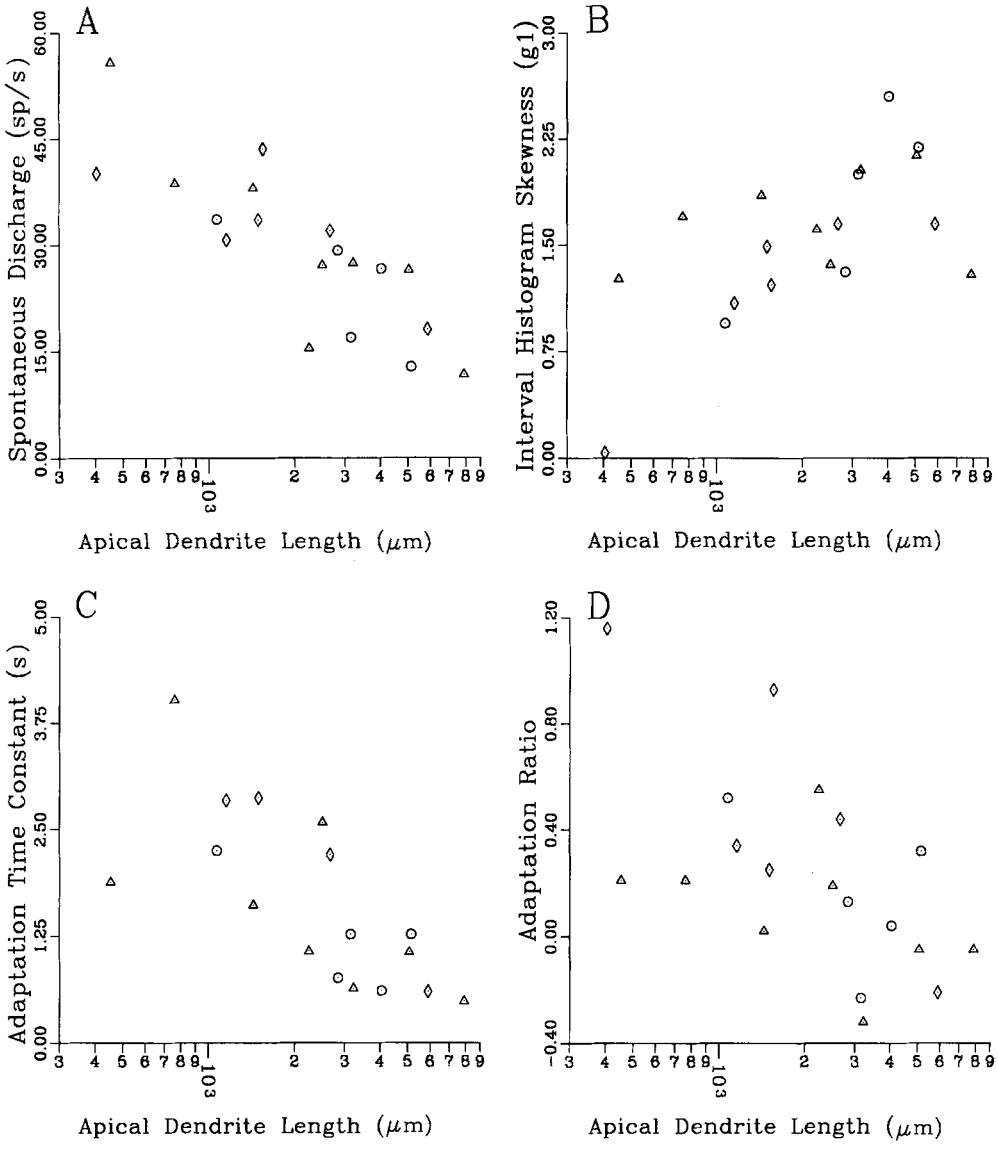

Fig. 9A–D. Plots showing the relationships between spontaneous firing frequency (**A**), interval histogram skewness (**B**), adaptation time constant (**C**), adaptation ratio (**D**) and apical dendrite size. Correlation coeffs. for the pooled data and for lateral segment cells, centrolateral cells, and centromedial cells analyzed independently are: **A** −0.83, −0.76, −0.87, −0.75; **B** 0.63, 0.86, 0.24, 0.9; **C** −0.72, −0.77, −0.66, −0.97; **D** −0.6, −0.5, −0.42, −0.83. $N=5$ for lateral segment cells, 8 for centrolateral cells, and 6 for centromedial cells. Two neurons, deep basilar pyramidal cells in the centromedial segment, showed no response adaptation, hence are not included in the plot of time constant versus dendrite length

decayed more slowly, and the cell maintained a significantly higher spike frequency throughout the stimulus. Although the response of the cell of Fig. 7B had a tonic component, the time course of its response differed from that of the DBP cells. The latter cells' responses show no adaptation at all to long-duration stimuli, instead the initial weak response builds over the first few seconds of stimulation.

Adaptation time constants were measured from the responses to 10 s increases in EOD amplitude as described in Methods. The degree of adaptation was also measured as the ratio of the spike frequency determined during the last 5 s of stimulation, minus the cell's resting frequency, to the change in spike frequency determined from the first second of the response. Data from cells that completely adapt produce ratios near zero, and data from tonic cells will give ratios near 1.0. The adaptation time constant for the cell of Fig. 7A was 0.49 s, and the adaptation ratio was −0.05. These measures were 2.25 s and 0.52, respectively for the cell of Fig. 7B, and the adaptation ratio for the DBP cell of Fig. 7C was 1.16. These measures were also strongly correlated with the size of a neuron's apical dendrite as shown in Fig. 9C, D. Correlation coefficients were −0.72 and −0.6 for time constant and adaptation ratio data, respectively, and significant correlations persisted when data from each ELL segment were analyzed separately.

These cells' spontaneous firing and adaptation characteristics are also correlated with the measurements of soma depth as expected from Fig. 7D. These correlations are generally weaker than those relating physiological characteristics to apical dendrite size, but they are all statistically significant ($P<0.02$).

Discussion

Horseradish peroxidase injections to the NPd such as shown in Fig. 1 preferentially label the deep basilar pyramidal (DBP) cells, and this may reflect a relatively exclusive projection of these cells to the ventral NPd. The preferential labeling of these cells may also be, at least in

part, a consequence of the larger diameter of DBP cell axons entering the NPd relative to those of the more superficial BP and NBP cells. HRP injections into the NPd typically result in dense and complete labeling of the deep cells, but the more superficial pyramidal cells are always weakly labeled. When similar injections are made in the torus semicircularis, both the deep and superficial pyramidal cells are strongly labeled despite the fact that transport distances are greater. Axons of DBP cells entering the NPd (Fig. 2A) had diameters averaging about 6 μm. Axons entering the NPd following an ELL injection that predominantly labeled the superficial pyramidal cells had diameters averaging 3.9 μm. ELL efferent axons branch in the lateral lemniscus near to where the fibers enter the NPd, and the diameters of these branches, labeled after a superficial ELL injection, are typically 40 to 60% of that of the parent axon which continues to the torus. Hence, the small diameter of the superficial BP and NBP cell axons that enter the NPd may limit the retrograde transport of HRP. It seems doubtful, however, that axon diameter differences alone could account for the near total absence of superficial pyramidal cell labeling following injections such as shown in Fig. 1, since more rostral NPd injections label a mixture of deep and superficial cell types.

In earlier studies of NPd efferent neurons we found tonically responding multipolar cells concentrated in the caudal-ventral region of the NPd. These cells, which probably receive major synaptic input from the DBP cells, gave short latency responses, averaging 5.7 ms, to excitatory stimuli (Bastian and Bratton 1990). Two additional categories of NPd neurons, stellate cells either excited or inhibited by increased EOD amplitude, responded phasically and with longer latencies, averaging 8.2 and 13.8 ms respectively (Bratton and Bastian 1990). The phasic responses of the stellate cells suggests that they are driven by the phasically responding BP and NBP cells, and if so, the longer latencies of the stellate cells could be due, in part, to an additional conduction delay associated with the thin axon branches of the phasic BP and NBP cells that enter the NPd.

Neuron morphology and physiological properties

The intracellular recording and labeling experiments show that the rate and degree of adaptation and the spontaneous activity patterns of the basilar pyramidal cells vary over a wide range. Furthermore, these physiological characteristics are highly correlated with both

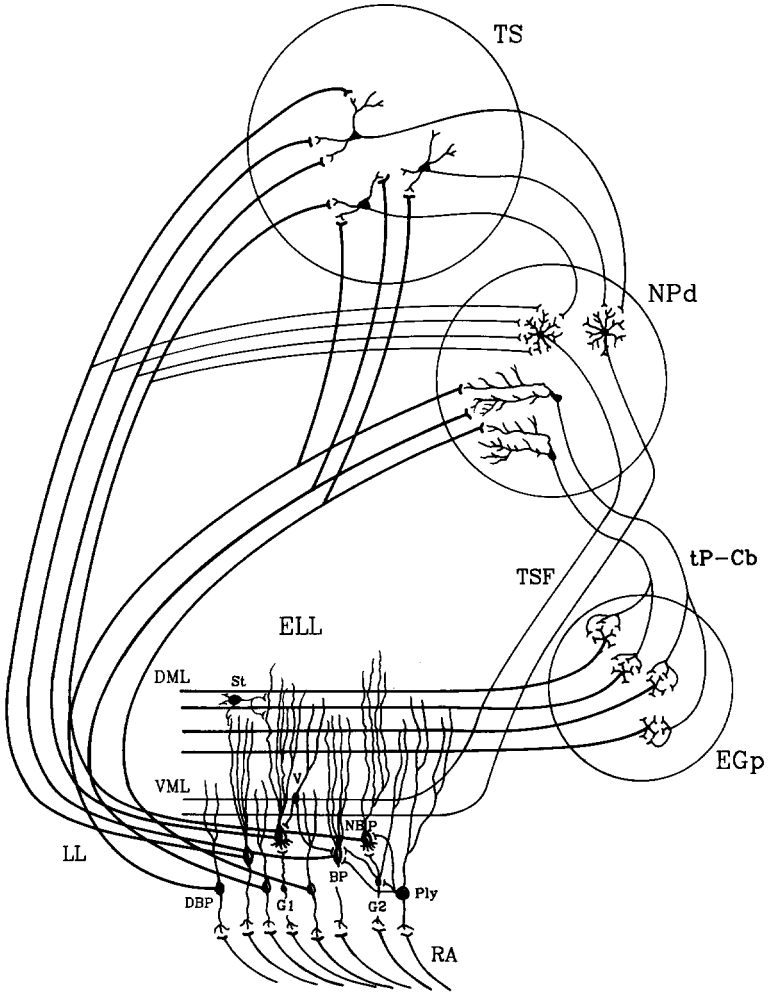

Fig. 10. Simplified diagram of the ELL and its connections with efferent targets and sources of descending input. *BP*, basilar pyramidal cell; *DBP*, deep basilar pyramidal cell; *DML*, dorsal molecular layer; *EGp*, posterior eminentia granularis; *ELL*, electrosensory lateral line lobe; *G1*, type 1 granule cell; *G2*, type 2 granule cell; *LL*, lateral lemniscus; *Ply*, polymorphic cell; *NBP*, nonbasilar pyramidal cell; *NPd*, nucleus praeeminentialis dorsalis; *RA*, receptor afferents; *St*, stellate cell, *tP–Cb*, tractus praeeminentialis cerebellaris; *TS*, torus semicircularis; *TSF*, tractus strati fibrosi; *V*, ventral molecular layer neuron; *VML*, ventral molecular layer

a neuron's apical dendrite size and the depth of the soma within the cellular laminae of the ELL. These morphological correlates probably indicate a functional relationship, but at this time we can only speculate as to how either apical dendrite size or soma placement might give rise to the physiological differences. A simplified diagram of the neural circuitry of the ELL and of its connections with other brain areas is shown in Fig. 10. Two separate, but not mutually exclusive, mechanisms can be proposed to account for the variability of basilar pyramidal cell responses:

The role of inhibitory interneurons. ELL inhibitory interneurons certainly contribute to the temporal response characteristics of ELL pyramidal cells. Stellate cells (St of Fig. 10) of both the dorsal and ventral molecular layers, shown to be GABAergic (Maler and Mugnaini, personal comm.), receive synaptic input from molecular layer parallel fibers and probably make inhibitory synapses with the apical dendrites of pyramidal cells as well as other ELL inhibitory interneurons (Maler 1979; Maler et al. 1981). These cells are distributed in a regular pattern within the DML and VML, and they project locally within the molecular layers. It seems likely that larger apical dendritic trees would receive greater numbers of stellate cell synapses. The correlation between adaptation characteristics and apical dendrite size could, therefore, be explained as a consequence of increased stellate cell input to the more phasic cell types. The enhanced pyramidal cell excitability seen when DML input is reduced by lesions of the EGp or by local anesthetic injection (Bastian 1986a) could also be explained as a result of decreased stellate cell input.

The direct ELL molecular layer parallel fiber inputs to pyramidal cell apical dendrites is also expected to alter excitability and perhaps influence spontaneous firing characteristics. The enormous differences in the basilar pyramidal cells' apical dendritic trees should determine the degree to which these cells are influenced by descending inputs, particularly input to the dorsal molecular layer. The phasically responding cells with the largest apical dendrites are expected to form numerous synaptic contacts with the DML parallel fibers, while the tonically responding deep pyramidal cells with their short apical dendrites receive little or no DML input. The parallel fiber to pyramidal cell synapse is, however, almost certainly excitatory. The parallel fibers probably use glutamate as the neurotransmitter (Nadi and Maler 1987) and kainic acid, quisqualate and NMDA receptors are found in the ELL molecular layers (Maler and Monoghan 1989). Direct electrical stimulation of parallel fibers in an 'in vitro' ELL preparation evokes excitatory responses in pyramidal cells (Mathieson and Maler 1988; Turner and Maler 1989). Given that these synapses are excitatory, decreased activity in the NPd–EGp–DML pathway, as caused by EGp lesions, would be predicted to cause reduced pyramidal cell excitability instead of the increased excitability that has been observed.

Slow afterpotentials or afterhyperpolarizations resulting from potassium conductances, including Ca^{++}-mediated K^+ conductance, are known to be determinants of spike frequency adaptation and can markedly decrease a neuron's excitability (Schwindt et al. 1988a, b; Mason and Larkman 1990). Calcium activated K^+ currents have also been shown to arise subsequent to NMDA receptor activation and the resulting inward Ca^{++} current (Hill et al. 1989; Hablitz and Mistry 1990). NMDA receptors are found in both the DML and VML, and Mathieson and Maler (1988) have shown that Ca^{++} activated K^+ conductances are operative in a subset of ELL pyramidal cells. This suggests that perhaps some component of the pyramidal cell adaptation characteristics might be a consequence of Ca^{++} activated K^+ conductances following NMDA receptor activation. However, preliminary experiments in which the calcium chelator EGTA was iontophoresed into phasic pyramidal cells caused no marked change in temporal response characteristics.

The neurons of the ventral molecular layer (V of Fig. 10), the type II granule cells (G2), and the polymorphic cells (Ply) all have apical dendrites extending into the ELL molecular layers and provide inhibitory input to pyramidal cells as shown in Fig. 10 (Maler et al. 1981). The type II granule cells and the polymorphic cells also receive receptor afferent input and contribute to antagonistic surrounds of pyramidal cell receptive fields (Maler et al. 1981; Shumway and Maler 1989). Feedforward inhibition mediated by such interneurons receiving receptor afferent input should contribute to the phasic response characteristics of the pyramidal cells. The duration of the decreased pyramidal cell excitability due to this inhibition will depend on the timecourse of the interneurons' responses to changes in receptor afferent input. Presently, no direct information regarding the inhibitory interneurons' physiological characteristics are available.

Activity in the NPd–EGp–DML pathway is also expected to excite these inhibitory interneurons thereby further decreasing pyramidal cell responsiveness. This descending input to the inhibitory neurons may be the principle source of the long-term changes in excitability we refer to as gain control. It is known that the input to the EGp–DML pathway, the multipolar cells of the NPd, respond tonically, so that inhibition mediated by this descending circuit may also be tonic (Bastian and Bratton 1990). This idea is reinforced by the results of experiments using lesions or anesthetics to reduce activity in the NPd–EGp–DML pathway. These treatments result in permanently increased pyramidal cell excitability (Bastian 1986a, b). Maler and Mugnaini (1986) have demonstrated a high density of GABAergic synapses in the polymorphic and granular layers of the ELL, and studies in which the GABA antagonist bicuculline was injected into the ELL resulted in enhanced pyramidal cell sensitivity and increased adaptation time constants similar to the effects due to reduced input to the DML (Shumway and Maler 1989). Hence, GABAergic inhibition mediated by inhibitory interneurons driven by both receptor afferent and descending inputs probably accounts for a significant portion of the pyramidal cells' adaptation.

The correlation between pyramidal cell response characteristics and apical dendrite size is not explained

by mechanisms based on the activity of the polymorphic or granule type II inhibitory interneurons. The pyramidal cell physiological characteristics are, however, also correlated with soma positions within the ELL cellular laminae, and soma position may reflect the type and density of inhibitory synaptic inputs to pyramidal cells (Maler, personal comm.). It is necessary to assume that the deep basilar pyramidal cells receive far fewer inhibitory inputs than do the more superficial pyramidal cells since the former show nonadapting responses. The fact that the superficial pyramidal cells have prominent somatic dendrites whereas the deep cells have none may reflect these postulated differences in inhibitory inputs.

Intrinsic membrane properties. Morphological variations in apical dendrite size will be related to differences in the passive cable properties of these neurons and may also indicate different types and densities of ligand gated channels. Differences in single-cell morphology within populations of neurons serving the same general function can be linked to different intrinsic membrane properties as has been shown for pyramidal neurons in rat visual cortex (Larkman and Mason 1990; Mason and Larkman 1990). This in vitro study showed that neurons categorized according to depth within the cortex, apical dendritic size, and several other morphological measures, differed in membrane time constant, spike frequency versus injected current relationships, and response adaptation. The ELL has also been studied in vitro (Mathieson and Maler 1988), and pyramidal cells fell into two classes based on their responses to depolarizing current injection. Roughly 2/3 of the pyramidal cells responded tonically to depolarizing current injection while the remaining cells produced rapidly adapting responses. The differences in these response types was shown to be due to the presence of a calcium dependent potassium conductance, gK(Ca), in the phasically responding cells. The phasic responses could be converted to the tonic type by incubating the preparation in the gK(Ca) blocker apamin or by injecting the Ca^{++} chelator EGTA into the pyramidal cell through the recording pipette. These treatments had minimal effects on the tonically responding cells. The cells showing the different response patterns were not identified morphologically so it is not known if the intrinsically tonic cell type corresponds to the deep basilar pyramidal cells of this study. Additional in vitro studies in which single cells are stained are needed to determine if major differences in membrane properties can be correlated with morphological differences such as apical dendrite size.

Variations in response properties among ELL segments

Recent studies (Shumway 1990a, b) demonstrated that several physiological and anatomical characteristics of ELL pyramidal cells varied with a cell's location among the ELL segments or maps. Adaptation time constants were measured and these were, on average, shortest in the lateral map, longer in the centrolateral map, and longest in the centromedial map. The physiological responses were recorded extracellularly, hence no anatomical measurements are available for comparison with the results of this study.

Our results provide morphological correlates of the variations in temporal response characteristics and show that neurons having responses ranging from very phasic to totally tonic are found within each of the lateral 3 ELL segments. Shumway (1990a) also saw considerable variation in response characteristics among cells from a given segment, hence those results reflect statistical differences among the populations of cells within each segment. The sample of intracellularly labeled cells in this study is smaller than that of Shumway (1990a), and the cells that we studied do not comprise a random sample. We tried to record from and label cells that spanned a wide range of adaptation characteristics and many of the more easily impaled superficial pyramidal cells were passed while searching for the deep basilar pyramidal cells. Despite these biases, the average time constants from each of the segments follow the same pattern as reported by Shumway (1990a). The adaptation time constant of lateral segment cells averaged 1.2 s, that of the centrolateral cells averaged 1.6 s, and that of the centromedial segment averaged 2.6 s. These were not significantly different as judged by analysis of variance.

The time constants reported here for ELL pyramidal cells ranged from about 50 ms to in excess of 4 s and are much longer than those reported earlier, which ranged from about 10 to 200 ms (Bastian 1981, 1986a, b; Shumway and Maler 1989; Shumway 1990a). The difference is solely due to the methods used. In the earlier studies, time constants were measured from PSTHs in which responses to repeated presentations of brief (100 to 300 ms duration) changes in EOD amplitude are accumulated. Since these cells fire in a phase locked manner to the transient portion of the stimulus, the initial peak of the histogram is accentuated. Time constants measured from these are shorter than those measured from single stimulus presentations such as shown in Fig. 8C and F. That the difference was methodological was verified by computing adaptation time constants from the PSTHs for each cell of this study when sufficient data were available (17 of 19 cases). These ranged from 2 to 50 ms and were also significantly correlated with the size of the cells' apical dendrites ($r = -0.49$). The correlations remained significant when cells from each segment were analyzed separately.

Gain control and the deep basilar pyramidal cells

The deep basilar pyramidal cells are critical components of a feedback loop that adjusts the gain or sensitivity of the phasically responding pyramidal cells. Figure 10 summarizes the major connections between the ELL, its efferent targets, and the sources of its feedback connections. In normal fish, basilar pyramidal cells produce nearly constant-sized responses to electrolocation targets despite reductions of EOD amplitude of as much as 40%. Reductions in EOD amplitude decrease the size of the electrosensory stimulus caused by a given target and reduce the change in receptor afferent firing frequency.

The constant pyramidal cell responses suggested that a gain control mechanism was operating within the electrosensory system which could compensate for the reduced receptor afferent input. When the EGp is lesioned, however, pyramidal cells lose the ability to maintain constant-sized responses when EOD amplitude is reduced (Bastian 1986b).

These results led to the suggestion that normal levels of activity in the NPd–EGp–DML circuit hold BP and NBP cell excitability at a reduced value and that excitability could be modulated upward when the sensory system detects reduced electric organ discharge amplitude, i.e., gain is increased.

Perhaps the simplest way to control the postulated changes in pyramidal cell excitability would be to use a tonic measure of EOD amplitude as the signal to adjust system gain. The NPd is the most likely source of this control signal since it provides the major electrosensory input to the EGp (Sas and Maler 1987). Intracellular recording and labeling studies showed that the NPd multipolar neurons have precisely the properties required to adjust pyramidal cell sensitivity (Bastian and Bratton 1990). Their responses to long-term changes in EOD amplitude are tonic, they signal changes in EOD amplitude with high resolution, and they show relatively poor sensitivity to moving electrolocation targets as compared to other types of electrosensory neurons. That these neurons project to the EGp was shown by both retrograde transport of HRP (Sas and Maler 1987) and by lucifer yellow staining of these cells during the physiological studies.

The tonic responses of the multipolar neurons raised a question as to their source of input. The principal electrosensory afferents to the NPd come directly from the ELL or from the torus semicircularis, which receives its electrosensory input from the ELL. The known categories of ELL output neurons that encode EOD amplitude, the basilar and nonbasilar pyramidal cells, generate phasic responses (Enger and Szabo 1965; Bastian 1981; Saunders and Bastian 1984; Shumway 1990a). Recordings from NPd afferent fibers having tonic response properties suggested, however, that a subset of ELL neurons may be specialized to provide the tonic measures of EOD amplitude to the multipolar cells (Bastian and Bratton 1990). The deep basilar pyramidal cells, DBP cells of Fig. 10, have physiological properties identical to those of the axon terminals recorded from in the NPd. Electron microscopic studies are needed to determine which NPd cell types receive synaptic input from the DBP cells, but at this time these are the best candidates for transmitting information about the steady-state amplitude of the EOD to the NPd multipolar cells.

The apical dendrites of the deep basilar pyramidal cells are very short and probably receive little if any DML input. If direct DML parallel fiber input to pyramidal cell apical dendrites is a functional component of the gain control circuitry, then these cells' sensitivity will remain unchanged even when that of the superficial BP and NBP cells is altered. The DBP cells can be thought of measuring the true or absolute amplitude of the EOD while the more superficial cells encode a given relative change with a response which is, within limits, independent of absolute amplitude.

Both the superficial and deep cells are likely to receive inputs from the VML fibers, and a recent study has shown that a major category of NPd neurons, called stellate cells, project directly to the VML, and are not spontaneously active, hence they cannot provide any information about steady-state EOD amplitude. Rather, stellate cells are strongly driven by moving electrolocation targets as well as other short-term changes in EOD amplitude. It has been suggested that these cells alter the sensitivity of local populations of ELL neurons, perhaps altering receptive field properties or enhancing the neural representation of important stimuli relative to less important background stimuli (Bratton and Bastian 1990). Thus far, however, there has been no clear demonstration of the role of the VML in electrosensory processing.

Acknowledgements: We thank Drs. L. Maler and R. Turner for many helpful discussions and for the opportunity to examine unpublished anatomical data. Supported by NIH grant NS12337 and OCAST contract 1669.

References

Bastian J (1981a) Electrolocation I: An analysis of the effects of moving objects and other electrical stimuli on the electroreceptor activity of *Apteronotus albifrons*. J Comp Physiol 144:465–479

Bastian J (1981b) Electrolocation II: The effects of moving objects and other electrical stimuli on the activities of two categories of posterior lateral line lobe cells in *Apteronotus albifrons*. J Comp Physiol 144:481–494

Bastian J (1986a) Gain control in the electrosensory system mediated by descending inputs to the electrosensory lateral line lobe. J Neurosci 6:553–562

Bastian J (1986b) Gain control in the electrosensory system: a role for the descending projections to the electrosensory lateral line lobe. J Comp Physiol A 158:505–515

Bastian J (1986c) Electrolocation: Behavior, anatomy and physiology. In: Bullock TH, Heiligenberg W (eds) Electroreception. Wiley, New York, pp 577–612

Bastian J (1990) Electroreception. In: Stebbins WC, Berkley MA (eds) Comparative perception, complex signals, vol II. Wiley, New York, pp 35–89

Bastian J, Bratton B (1990) Descending control of electroreception. I. Properties of nucleus praeeminentialis neurons projecting indirectly to the electrosensory lateral line lobe, J Neurosci 10:1226–1240

Bratton B, Bastian J (1990) Descending control of electroreception II: Properties of nucleus praeeminentialis neurons projecting directly to the electrosensory lateral line lobe. J Neurosci 10:1241–1253

Carr CE, Maler L (1986) Electroreception in gymnotiform fish: Central anatomy and physiology. In: Bullock TH, Heiligenberg W (eds) Electroreception. Wiley, New York, pp 319–373

Carr CE, Maler L, Heiligenberg W, Sas E (1981) Laminar organization of the afferent and efferent systems of the torus semicircularis of gymnotiform fish: Morphological substrates for parallel processing in the electrosensory system. J Comp Neurol 203:649–670

Carr CE, Maler L, Sas E (1982) Peripheral and central projections of the electrosensory nerves in gymnotiform fish. J Comp Neurol 211:139–153

Enger PS, Szabo T (1965) Activity of central neurons involved in electroreception in some weakly electric fish (Gymnotidae). J Neurophysiol 28:800–818

Hablitz JJ, Mistry DK (1990) NMDA-evoked outward currents in

cultured neocortical neurons using nystatin-perforated patch recordings. Soc Neurosci Abstr 16:1184

Heiligenberg W (1977) Principles of electrolocation and jamming avoidance. In: Braitenberg V (ed) Studies of Brain Function, vol 1. Springer, Berlin Heidelberg New York, pp 1–85

Heiligenberg W (1986) Jamming avoidance systems: Model systems for neuroethology. In: Bullock TH, Heiligenberg W (eds) Electroreception. Wiley, New York, pp 613–649

Heiligenberg WH, Dye J (1982) Labelling of electroreceptor afferents in a gymnotoid fish by intracellular injection of HRP: The mystery of multiple maps. J Comp Physiol 148:287–296

Hill RH, Brodin L, Grillner S (1989) Activation of N-methyl-D-aspartate (NMDA) receptors augments repolarizing responses in lamprey spinal neurons. Brain Res 499:388–392

Larkman A, Mason A (1990) Correlations between morphology and electrophysiology of pyramidal neurons in slices of rat visual cortex. I. Establishment of cell classes. J Neurosci 10:1407–1414

Maler L (1979) The posterior lateral line lobe of certain gymnotoid fish: Quantitative light microscopy. J Comp Neurol 183:323–364

Maler L, Monoghan D (1989) Distribution of glutamate receptors in the electrosensory system of gymnotiform fish. Soc Neurosci Abstr 15:1135

Maler L, Mugnaini E (1986) Immunohistochemical identification of GABAergic synapses in the electrosensory lateral line lobe of a weakly electric fish *(Apteronotus leptorhynchus)*. Soc Neurosci Abstr 12:312

Maler L, Sas EKB, Rogers J (1981) The cytology of the posterior lateral line lobe of high-frequency weakly electric fish (Gymnotidae): Dendritic differentiation and synaptic specificity in a simple cortex. J Comp Neurol 195:87–139

Maler L, Sas E, Carr C, Matsubara J (1982) Efferent projections of the posterior lateral line lobe in gymnotiform fish. J Comp Neurol 211:154–164

Mason A, Larkman A (1990) Correlations between morphology and electrophysiology of pyramidal neurons in slices of rat visual cortex. II. Electrophysiology. J Neurosci 10:1415–1428

Mathieson WB, Maler L (1988) Morphological and electrophysiological properties of a novel in vitro preparation: The electrosensory lateral line lobe brain slice. J Comp Physiol A 163:489–506

Metcalf WK (1985) Sensory neuron growth cones comigrate with posterior lateral line lobe primordial cells in zebrafish. J Comp Neurol 238:218–224

Nadi S, Maler L (1987) The laminar distribution of amino acids in the caudal cerebellum and electrosensory lateral line lobe of weakly electric fish (Gymnotidae). Brain Res 425:218–224

Réthelyi M, Szabo T (1973) Neurohistological analysis of the lateral line lobe in a weakly electric fish, *Gymnotus carapo* (Gymnotidae, Pisces). Exp Brain Res 18:323–339

Sas E, Maler L (1983) The nucleus praeeminentialis: A Golgi study of a feedback center in the electrosensory system of gymnotid fish. J Comp Neurol 221:127–144

Sas E, Maler L (1987) The organization of afferent input to the caudal lobe of the cerebellum of the gymnotid fish *Apteronotus leptorhynchus*. Anat Embryol 177:55–79

Saunders J, Bastian J (1984) The physiology and morphology of two types of electrosensory neurons in the weakly electric fish *Apteronotus leptorhynchus*. J Comp Physiol A 154:199–209

Schwindt PC, Spain WJ, Foehring RC, Stafstrom CE, Chubb MC, Crill WE (1988a) Multiple potassium conductances and their functions in neurons from cat sensorimotor cortex in vitro. J Neurophysiol 59:424–449

Schwindt PC, Spain WJ, Foehring RC, Chubb MC, Crill WE (1988b) Slow conductances in neurons from cat sensorimotor cortex in vitro and their role in slow excitability changes. J Neurophysiol 59:450–467

Shumway CA (1990a) Multiple electrosensory maps in the medulla of weakly electric gymnotiform fish. I: Physiological differences. J Neurosci 9:4388–4399

Shumway CA (1990b) Multiple electrosensory maps in the medulla of weakly electric gymnotiform fish. II: Anatomical differences. J Neurosci 9:4400–4415

Shumway CA, Maler L (1989) GABAergic inhibition shapes temporal and spatial response properties of pyramidal cells in the electrosensory lateral line lobe of gymnotiform fish. J Comp Physiol A 164:391–407

Sokal RR, Rohlf FJ (1981) Biometry. W. H. Freeman and Company, San Francisco, pp 114–117

Turner RW, Maler L (1989) Synaptic plasticity in the cerebellar parallel fiber projection to the electrosensory lateral line lobe of gymnotiform fish. Soc Neurosci Abstr 15:1135

Zakon HH (1986) The electroreceptive periphery. In: Bullock TH, Heiligenberg W (eds) Electroreception. Wiley, New York, pp 103–156